

Boson expansion techniques, the Pauli principle, and the quasiparticle random phase approximation phase transition

Jorge G. Hirsch,^{1,*} Peter O. Hess,^{1,†} and Osvaldo Civitarese^{2,‡}

¹*Instituto de Ciencias Nucleares, Universidad Nacional Autónoma de México, Apartado Postal 70-543, México 04510 Distrito Federal, México*

²*Departamento de Física, Universidad Nacional de La Plata, c.c. 67 1900, La Plata, Argentina*

(Received 29 May 1998; revised manuscript received 25 June 1999; published 26 October 1999)

The onset of instabilities, in the standard proton-neutron quasiparticle random phase approximation (QRPA), is investigated by using different boson mappings and trial states belonging to a representation of coherent states. The model describes pairing and proton-neutron interactions. It is shown that an exact mapping of the Hamiltonian is needed to describe correctly the QRPA phase transition, i.e., that the algebra of all operators participant in the Hamiltonian should be preserved by the boson mapping. Spurious components of the wave functions, which appear if the Pauli principle is violated, are isolated by construction.

[S0556-2813(99)05511-9]

PACS number(s): 21.60.Jz, 21.60.Fw, 23.40.Hc

I. INTRODUCTION

The quasiparticle random phase approximation (QRPA) method has been intensively used in the past to describe collective properties in terms of two-quasi-particle correlations. The method is an acceptable alternative to the otherwise nonaffordable exact diagonalization in a large basis and proved to be suitable for the microscopic description of like-particle (proton-proton and neutron-neutron) two-quasi-particle excitations in a highly correlated vacuum. The QRPA method was also extended to describe proton-neutron excitations and it was used at large to calculate charge-dependent excitations and exotic nuclear decays [1–4]. It is well known that, in general, the validity of the QRPA method is restricted to small amplitude motion around the BCS vacuum. It was shown that the renormalization of some components of the two-body interactions can introduce very large ground state correlations and breakdown the QRPA symmetries. The use of the random phase approximation (RPA) and the QRPA methods near “critical points” [5,6] was reviewed in the search of new approximations beyond mean field [7].

The main assumption of the QRPA(RPA) approximation is the smallness of the number of bosons n_b in the correlated vacuum, compared with the total number Ω of fermionic pairs which is allowed by the Pauli principle. Depending on the adopted Hamiltonian the quantity n_b can be rather large and the harmonic approximation fails. It was shown long ago [8] that the RPA is unable to compensate for the breakdown of the symmetry ($n_b = \langle b^\dagger b \rangle = 0$) because it is limited to generate rearrangements of the mean field. Therefore it can be argued that extensions of the QRPA method beyond mean field approaches are severely limited due to the nonperturbative nature of the large amplitude motion induced by abnor-

mally large ground state correlations.

The obvious way of showing the validity of the RPA (QRPA) type of approaches near breakdown is to compare their results with exact shell model results [9]. Unfortunately, large scale shell model calculations are not available yet for the cases of interest, e.g., for heavy nuclei. The use of boson expansion techniques to handle this problem was suggested in a series of papers, which deal with the collapse of the QRPA [10,11]. In the present work we focus our attention on the Dyson boson expansion method [5,12,13] and use it to illustrate the RPA phase transition associated to an schematic model Hamiltonian [14,15]. Effects due to the violation of the Pauli principle, in the context of the boson expansion of the wave functions, are explored by using exponential and polynomial expansion. Following the method of Refs. [10,16] we shall introduce a complex order parameter to determine the dependence of the phase-transition point upon the coupling constants of the Hamiltonian and to compute expectation values in the QRPA, the renormalized QRPA [7] and in the Dyson boson expansion method [5,12,13].

The analysis is based on the comparison between exact results, the results of the conventional QRPA and the ones obtained with the renormalized RPA (or renormalized QRPA) with the results obtained by using a boson mapping (Dyson boson mapping) which preserves the algebra of the operators appearing in the Hamiltonian. It is shown that the renormalized versions of the QRPA fail to describe the QRPA phase transition, while the complete Dyson mapping exhibits the features of the exact solution over all the range of parameters. It is also found that the adopted boson mapping, which is exact for the Hamiltonian and approximate for the wave functions, leads to a good description of the phase transition. Clearly, the combined way, namely, the complete boson mapping of the Hamiltonian and the approximate one of the wave functions, is a nonperturbative approach and it goes well beyond mean field, as the exact solution does.

The formalism is presented in Sec. II, where we define the Hamiltonian, the QRPA and renormalized QRPA expressions, and the Dyson boson mapping. In Sec. III we intro-

*Electronic address: hirsch@nuclecu.unam.mx

†Electronic address: hess@nuclecu.unam.mx

‡Electronic address: civitare@venus.fisica.unlp.edu.ar

duce the different approximations for the wave functions and in Sec. IV we present the results corresponding to the matrix elements calculated by using the approximations described in Sec. III. In Sec. V we present the results and the discussion. Conclusions are drawn in Sec. VI.

II. THE HAMILTONIAN

The Hamiltonian adopted for the present calculations includes a single particle term, both for protons and neutrons, a pairing interaction between like nucleons, and a proton-neutron two body interaction parametrized in terms of particle-hole and particle-particle channels [1,2]. This form of H has been used previously both in realistic and in schematic calculations [10,14–16].

The schematic Hamiltonian reads

$$H = H_p + H_n + H_{\text{res}}, \quad (1)$$

where

$$H_p = \sum_p e_p a_p^\dagger a_p - G_p S_p^\dagger S_p, \quad H_n = \sum_n e_n a_n^\dagger a_n - G_n S_n^\dagger S_n, \quad (2)$$

$$H_{\text{res}} = 2\chi \beta_J^- \cdot \beta_J^+ - 2\kappa P_J^- \cdot P_J^+. \quad (3)$$

In the above expression the following definitions were introduced:

$$S_p^\dagger = \sum_p a_p^\dagger a_p^\dagger / 2, \quad S_n^\dagger = \sum_n a_n^\dagger a_n^\dagger / 2, \quad (4)$$

$$\beta_J^- \cdot \beta_J^+ = \sum_{M=-J}^J (-1)^M \beta_{JM}^- (\beta_{J-M}^-)^\dagger, \quad (5)$$

$$P_J^- \cdot P_J^+ = \sum_{M=-J}^J (-1)^M P_{JM}^- (P_{J-M}^-)^\dagger, \quad (6)$$

$$\beta_{JM}^- = \sum_{i,j} \langle i | \mathcal{O}_{JM} | j \rangle a_i^\dagger a_j, \quad P_{JM}^- = \sum_{i,j} \langle i | \mathcal{O}_{JM} | j \rangle a_i^\dagger a_j^\dagger, \quad (7)$$

$$\mathcal{O}_{1M} = \sigma_M \tau^-, \quad \mathcal{O}_{00} = \tau^-, \quad (8)$$

$a_p^\dagger = a_{j_p m_p}^\dagger$ being the particle creation operator and $a_p^\dagger = (-1)^{j_p - m_p} a_{j_p -m_p}^\dagger$ its time reversal.

We shall consider the one-shell limit of this Hamiltonian. Pairing effects will be accounted for by a quasiparticle mean field, for protons and neutrons separately, represented by the BCS solutions of a separable monopole-pairing interaction [17].

This Hamiltonian has been used both for the description of Fermi ($\Delta J=0, \Delta T=\pm 1$) and Gamow-Teller ($\Delta J=1, \Delta T=\pm 1$) excitations and the corresponding transitions [10,11]. The solutions for $\Delta J=0$ have been studied in [10] while the case of Gamow-Teller excitations has been presented in Ref. [11]. For the sake of simplicity and without loss of general-

ity, we proceed with the case of $\Delta J=0$ transitions. In the BCS representation the quasiparticle proton-neutron pair operator has the form

$$A^\dagger = [\alpha_p^\dagger \otimes \alpha_n^\dagger]_{M=0}^{J=0}. \quad (9)$$

Thus, at the QRPA order of approximation and keeping in the Hamiltonian bilinear products of A^\dagger and A , we arrive at the expression [10]

$$H = \epsilon C + \lambda_1 A^\dagger A + \lambda_2 (A^\dagger A^\dagger + A A), \quad (10)$$

where the proton and neutron quasiparticle energies have been replaced by a common value ϵ . The operator C and the coupling constants λ_1 and λ_2 of Eq. (10) are defined by

$$C = \sum_{m_p} \alpha_{p m_p}^\dagger \alpha_{p m_p} + \sum_{m_n} \alpha_{n m_n}^\dagger \alpha_{n m_n}, \quad (11)$$

$$\lambda_1 = 4\Omega [\chi (u_p^2 v_n^2 + v_p^2 u_n^2) - \kappa (u_p^2 u_n^2 + v_p^2 v_n^2)], \quad (12)$$

$$\lambda_2 = 4\Omega (\chi + \kappa) u_p v_p u_n v_n, \quad (13)$$

where $2\Omega = (2j+1)$ is the degeneracy of the shell in a standard notation [17].

The QRPA treatment of this Hamiltonian [10] yields the eigenvalue

$$E_{\text{QRPA}} = [(2\epsilon + \lambda_1)^2 - (2\lambda_2)^2]^{1/2},$$

which vanishes for $2\lambda_2 = 2\epsilon + \lambda_1$. This result, which is also found in the exact solution of the model, does not appear in the renormalized QRPA treatment of Refs. [7,18]. The collapse of the QRPA excitation energy has also been found in the extension of the present model to a larger group representation [11]. In the following we describe this feature in terms of a phase transition mechanism of the sort discussed long ago by Lane *et al.* [8].

Along this line, we introduce a boson mapping of Eq. (10) which preserves the Pauli principle. The link with the phase-transition mechanism is established by introducing, in this boson basis, coherent states [12,13] and an order parameter [16].

To achieve this goal we have performed the Dyson mapping [12,13] of the Hamiltonian (10) by replacing the quasiparticle-pair operators by

$$(A^\dagger)_D = b^\dagger \left(1 - \frac{b^\dagger b}{2\Omega} \right), \quad (A)_D = b, \quad (C)_D = 2b^\dagger b, \quad (14)$$

where the index D refers to the Dyson mapping and proton-neutron bosons are denoted by b^\dagger or b . The operators b^\dagger and b are boson creation and annihilation operators, which obey exact boson commutation relations. The number of proton-neutron bosons, $n_b = \langle b^\dagger b \rangle$, is restricted by the condition $n_b \leq 2\Omega$, which guarantees that spurious nonphysical states [12,13] are excluded.

The transformed Hamiltonian corresponding to Eq. (10) is given by

$$\begin{aligned}
 H &= (2\epsilon + \lambda_1)b^\dagger b - \frac{\lambda_1}{2\Omega}b^{\dagger 2}b^2 + \lambda_2\left(1 - \frac{1}{2\Omega}\right)b^{\dagger 2}, \\
 & - \frac{\lambda_2}{\Omega}\left(1 - \frac{1}{2\Omega}\right)b^{\dagger 3}b + \frac{\lambda_2}{4\Omega^2}b^{\dagger 4}b^2 + \lambda_2b^2.
 \end{aligned} \tag{15}$$

While the above form of the Hamiltonian is not Hermitian, due to the use of the non-Hermitian Dyson mapping, it has the advantage of having a finite number of terms allowing its exact diagonalization as well as a simple comparison with the other approximate expressions for H .

Notice that in the limit $2\Omega \rightarrow \infty$ we obtain the simplest quasiboson image [12] of the QRPA Hamiltonian

$$H_{\text{QRPA}} = (2\epsilon + \lambda_1)b^\dagger b - \lambda_2(b^{\dagger 2} + b^2). \tag{16}$$

The QRPA approximation relies upon the assumption that in the commutator

$$[A, A^\dagger] = \left(1 - \frac{b^\dagger b}{\Omega}\right), \tag{17}$$

terms of the order of $1/\Omega$ are neglected. This is the so-called quasiboson approximation. The renormalized QRPA approach aims to include these terms by substituting the number operator ($\hat{n}_b = b^\dagger b$) by n_b at the level of the QRPA equations of motion. The boson mapping of the Hamiltonian, keeping terms as done in the renormalized QRPA, is given by

$$H_{\text{RQRPA}} = \left[2\epsilon + \lambda_1\left(1 - \frac{\hat{n}_b}{\Omega}\right)\right]b^\dagger b + \lambda_2\left(1 - \frac{\hat{n}_b}{\Omega}\right)(b^{\dagger 2} + b^2). \tag{18}$$

Replacing $\hat{n}_b \rightarrow n_b$ and holding the relation (17), at the expectation value level, terms of the type n_b/Ω will appear in the Hamiltonian (18) which are twice larger than the corresponding ones of Eq. (15).

III. APPROXIMATIONS FOR THE TRIAL STATES

After performing the boson mapping we shall introduce trial states, which are related to coherent states [12,13]. For convenience we shall call them, in general, coherent states. As a first approximation we chose

$$|\alpha\rangle = N_0 \sum_{l=0}^{2\Omega} \frac{\alpha^l}{l!} b^{\dagger l} |0\rangle = N_0 \sum_{l=0}^{2\Omega} \frac{\alpha^l}{\sqrt{l!}} |l\rangle, \tag{19}$$

where α is a complex variable, N_0 is a normalization factor, and $|l\rangle = \frac{b^{\dagger l}}{\sqrt{l!}}|0\rangle$, with $b|0\rangle = 0$ and $\langle l|l'\rangle = \delta_{ll'}$. The upper value $l = 2\Omega$ in the sum of Eq. (19) guarantees that the Pauli principle is observed in the boson expansion of the states $|\alpha\rangle$.

We will also use an approximation simpler than the previous one which allows for any number of bosons, thus it does not take into account the Pauli principle. This trial state is defined as

$$|\alpha_\infty\rangle = N_\infty \sum_{l=0}^{\infty} \frac{\alpha^l}{l!} b^{\dagger l} |0\rangle = N_\infty \sum_{l=0}^{\infty} \frac{\alpha^l}{\sqrt{l!}} |l\rangle. \tag{20}$$

Since the Dyson boson mapping is non-Hermitian we have to deal with bra ($\langle\alpha|$) and ket ($|\tilde{\alpha}\rangle$) states, namely,

$$\begin{aligned}
 \langle\alpha| &= \langle 0|N_0 \sum_{l=0}^{2\Omega} \frac{\alpha^{*l}}{l!} (A)_D^l = \langle 0|N_0 \sum_{l=0}^{2\Omega} \frac{\alpha^{*l}}{l!} b^l, \\
 |\tilde{\alpha}\rangle &= \tilde{N}_0 \sum_{l=0}^{2\Omega} \frac{\alpha^l}{l!} (A^\dagger)_D^l |0\rangle \\
 &= \tilde{N}_0 (2\Omega!) \sum_{l=0}^{2\Omega} \left[\frac{\alpha}{2\Omega}\right]^l \frac{(b^\dagger)^l}{l!(2\Omega-l)!} |0\rangle.
 \end{aligned} \tag{21}$$

The Hamiltonian (15) can connect states with even (odd) number of pairs, only. Therefore, we can split the sums of Eq. (21) into even and odd parts. The corresponding contributions will be denoted by subscripts e (for even) and o (for odd), respectively.

IV. MATRIX ELEMENTS

The expectation value of the transformed Hamiltonian, Eq. (15), gives the potential energy surface $E(\alpha) = E_r + iE_i$, which depends both on the real and imaginary parts of the order parameter $\alpha = \rho e^{i\theta}$ as well as on the actual value of the coupling constants of the model [16]. The minima of this potential energy surface can be identified by performing a variation of the order parameter for different values of χ and κ . Different regimes of the solution will therefore be determined by nontrivial values of the order parameter.

In the following we have summarized the expressions needed to calculate expectation values in the different approximations, namely,

$$\langle\alpha_i|(b^\dagger)^{n_1} b^{n_2}|\tilde{\alpha}_i\rangle = N_i \tilde{N}_i (2\Omega)! e^{i(n_2 - n_1)\theta} \frac{\rho^{n_1 + n_2}}{(2\Omega)^{n_2}} g_{n_1 n_2}^{(i)}(\rho), \tag{22}$$

where $|\alpha_i\rangle$ reads for $|\alpha\rangle$, $|\alpha_e\rangle$, and $|\alpha_o\rangle$ and

$$g_{n_1 n_2}^{(i)}(\rho) = \sum_{l=l_{\min}}^{l_{\max}} \left(\frac{\rho^2}{2\Omega}\right)^l \frac{1}{l!(2\Omega - l - n_2)!}, \tag{23}$$

where $l_{\max} = \min(2\Omega - n_1, 2\Omega - n_2)$, and in Eqs. (22) and (23) we have included for brevity three different cases: $g_{n_1 n_2}(\rho)$, without superscript, corresponds to the trial state in which all number of bosons are allowed and the index l takes all integer values starting at $l_{\min} = 0$; $g_{n_1 n_2}^{(e)}(\rho)$ is associated with the trial state with even number of bosons, the l can have only even values larger than l_{\min}

$= \text{mod}(n_1, 2)$; $g_{n_1 n_2}^{(o)}$ is related with the trial state with odd number of bosons, with l having only odd values larger than $l_{\min} = \text{mod}(n_1, 2) + 1$.

The following quantities are also needed [16]:

$$\langle \alpha | (b^\dagger)^{n_1} b^{n_2} | \alpha \rangle = N_0^2 e^{i(n_2 - n_1)\theta} \rho^{n_1 + n_2} h_n(\rho), \quad (24)$$

with

$$h_n \equiv h_{\text{Min}(n_1, n_2)}(\rho) = \sum_{l=0}^{2\Omega-n} \frac{\rho^{2l}}{l!}. \quad (25)$$

For the exponential approximation we have obtained

$$\langle \alpha | (b^\dagger)^{n_1} b^{n_2} | \alpha \rangle = e^{i(n_2 - n_1)\theta} \rho^{n_1 + n_2}. \quad (26)$$

Notice that the factors $g_{n_1 n_2}^{(i)}$ of Eq. (23) have a rather involved dependence on n_1 and n_2 while Eq. (26) has a simpler structure. In this way we have a complete family of trial states of different complexity, which are available to compute the expectation value of the Hamiltonian.

We use a variational procedure to obtain the minimum for the real part of the expectation value of the Hamiltonian. It has the form

$$\begin{aligned} \frac{\langle \alpha | H | \tilde{\alpha} \rangle}{\langle \alpha | \tilde{\alpha} \rangle} &= \left[(2\epsilon + \lambda_1) \frac{g_{11}}{g_{00}} + \frac{\lambda_2}{2\Omega} \cos(2\theta) \frac{g_{02}}{g_{00}} \right. \\ &+ (2\Omega - 1) \frac{g_{20}}{g_{00}} \frac{\rho^2}{2\Omega} - \left. \left[\frac{\lambda_1}{2\Omega} \frac{g_{22}}{g_{00}} \right. \right. \\ &+ \lambda_2 \cos(2\theta) \left. \left(1 - \frac{1}{2\Omega} \right) \frac{g_{31}}{g_{00}} \right] \frac{\rho^4}{(2\Omega)^2} \\ &+ \left. \lambda_2 \cos(2\theta) \frac{g_{42}}{g_{00}} \frac{\rho^6}{(2\Omega)^4} \right]. \quad (27) \end{aligned}$$

Similar results are obtained for the trial state with only even or odd values of l by replacing $g_{ij} \rightarrow g_{ij}^{(e(o))}$.

If the same trial state (19) is used both for the bra and the ket, paying no attention to the fact the H is not Hermitian in the bosonic basis as it was done in [16], the following expectation value of H is obtained:

$$\begin{aligned} \langle \alpha | H | \alpha \rangle &= \left[(2\epsilon + \lambda_1) \frac{h_1}{h_0} + \lambda_2 \cos(2\theta) \left(2 - \frac{1}{2\Omega} \right) \frac{h_2}{h_0} \right] \rho^2 \\ &- \left[\frac{\lambda_1}{2\Omega} \frac{h_2}{h_0} + \frac{\lambda_2 \cos(2\theta)}{\Omega} \left(1 - \frac{1}{2\Omega} \right) \frac{h_3}{h_0} \right] \rho^4 \\ &+ \frac{\lambda_2 \cos(2\theta)}{(2\Omega)^2} \frac{h_4}{h_0} \rho^6. \quad (28) \end{aligned}$$

For the exponential trial state we obtain

$$\begin{aligned} \langle \alpha_\infty | H | \alpha_\infty \rangle &= \left[(2\epsilon + \lambda_1) + \lambda_2 \cos(2\theta) \left(2 - \frac{1}{2\Omega} \right) \right] \rho^2 \\ &- \left[\frac{\lambda_1}{2\Omega} + \frac{\lambda_2 \cos(2\theta)}{\Omega} \left(1 - \frac{1}{2\Omega} \right) \right] \rho^4 \\ &+ \frac{\lambda_2 \cos(2\theta)}{(2\Omega)^2} \rho^6. \quad (29) \end{aligned}$$

The expectation value of the Hamiltonian H_{QRPA} (16) between purely exponential coherent states is given by

$$\langle \alpha_\infty | H_{\text{QRPA}} | \alpha_\infty \rangle = [(2\epsilon + \lambda_1) + 2\lambda_2 \cos(2\theta)] \rho^2. \quad (30)$$

This quadratic dependence on ρ shows that H_{QRPA} is the harmonic approximation of Hamiltonian (15). As it is well known, this approximation is valid as long as the minimum of the effective potential is located at $\rho=0$ but it fails in the presence of a phase transition. This expectation value can be seen as the result of the trivial substitution of the operators A^\dagger, A in Eq. (2) by the complex numbers $\rho e^{i\theta}, \rho e^{-i\theta}$.

In a similar way the expectation value of the Hamiltonian of the renormalized QRPA of Eq. (18) in the state (19) is given by

$$\begin{aligned} \langle \alpha | H_{\text{RQRPA}} | \alpha \rangle &= \left[(2\epsilon + \lambda_1) \frac{h_1}{h_0} + 2\lambda_2 \cos(2\theta) \frac{h_2}{h_0} \right] \rho^2 \\ &- \left[\frac{\lambda_1}{\Omega} \left(\frac{h_1}{h_0} \right)^2 + \frac{2\lambda_2 \cos(2\theta)}{\Omega} \frac{h_1 h_2}{h_0^2} \right] \rho^4. \quad (31) \end{aligned}$$

The comparison between Eqs. (28) and (31) shows the exact and renormalized QRPA results deviate, due to differences in the coefficient of ρ^4 . In order to complete this section, and for later use, we show the expressions corresponding to Fermi transitions [10] between coherent states.

As an example we show the results obtained with Dyson trial states. The mapping of the operator β^- reads

$$\beta^- = u_p v_n (A^\dagger)_D + v_p u_n (A)_D = u_p v_n b^\dagger \left(1 - \frac{b^\dagger b}{2\Omega} \right) + v_p u_n b, \quad (32)$$

and the matrix elements are written

$$\begin{aligned} \langle \alpha | \beta^- | \tilde{\alpha} \rangle &= \sqrt{N_0 \tilde{N}_0} (2\Omega - 1)! \rho e^{-i\theta} g_{01}(\rho) (u_p v_n \\ &+ e^{2i\theta} v_p n_n) \quad (33) \end{aligned}$$

and

$$\begin{aligned} \langle \alpha_o | \beta^- | \tilde{\alpha}_e \rangle &= \sqrt{N_o \tilde{N}_e} (2\Omega - 1)! \rho e^{-i\theta} [u_p v_n g_{21}^{(e)}(\rho) \\ &+ e^{2i\theta} v_p n_n g_{11}^{(e)}(\rho)]. \quad (34) \end{aligned}$$

In Eq. (34) the operator β^- connects states with even and odd number of bosons, while in Eq. (33) the trial state contains both even and odd powers of b^\dagger .

V. RESULTS AND DISCUSSION

In the following we will present numerical results which correspond to the choice of the model parameters [Eqs. (10) and (13)]:

$$\Omega = 5, \quad N_p = 4, \quad N_n = 6, \quad \epsilon = 1.0 \text{ MeV}, \quad \chi = 0. \quad (35)$$

The quantities N_p and N_n are the number of active protons and neutrons, respectively, considered in the BCS equations. The particle-particle (proton-neutron) strength κ is varied in the range $0 \leq \kappa \leq 0.2$ MeV. Inserting these numerical values in Eq. (13) the parameters in the Hamiltonian (10) take the simple form $\lambda_1 = -9.6\kappa, \lambda_2 = 4.8\kappa$.

The potential-energy surface $\langle H \rangle$ was minimized as a function of the complex order parameter $\alpha = \rho e^{i\theta}$. In all the cases presented in the previous section the dependence of $\langle H \rangle$ on θ is given by

$$\langle H \rangle = \mathcal{A}(\rho) + \mathcal{B}(\rho) \cos(2\theta) \quad (36)$$

and the extremum is determined by

$$\frac{\partial}{\partial \theta} \langle H \rangle = -2\mathcal{B}(\rho) \sin(2\theta) = 0, \quad (37)$$

which implies that at the minimum

$$\cos(2\theta) = \pm 1. \quad (38)$$

The value which provides a minimum in ρ is $\cos(2\theta) = -1$, which is the one we will use in the rest of this article.

The critical behavior of the potential-energy surfaces is shown in Fig. 1. We denote the expectation value $\langle \alpha_\infty | H_{\text{QRPA}} | \alpha_\infty \rangle$ as ‘‘QRPA,’’ $\langle \alpha_\infty | H | \alpha_\infty \rangle$ as ‘‘exponential,’’ $\langle \alpha | H | \alpha \rangle$ as ‘‘Ref. [16],’’ and $\langle \alpha | H | \tilde{\alpha} \rangle$ as ‘‘Dyson.’’ Figure 1 [insets (a), (b), and (c)] shows the results for $\kappa = 0, 0.1$ and 0.2 MeV, respectively. In inset (a) of Fig. 1 we have $\lambda_1 = \lambda_2 = 0$, for which the Hamiltonian is quadratic in b^\dagger and b . Due to this fact the expectation values of H_{QRPA} and H coincide exactly when the exponential approximation is used. However, the other two approximations take into account the Pauli principle at the level of the wave function and exhibit a saturation at $n_b = 2\Omega$, with the asymptotic value ($\rho \rightarrow \infty$) $\langle \alpha | H | \alpha \rangle = 2\epsilon n_b$. For $\kappa = 0.1$ MeV, Inset (b) of Fig. 1, the QRPA curve is still a parabola, but with nearly vanishing curvature. The other three curves are very similar up to $\rho \sim 2.0$. Beyond that point the exponential curve has a maximum and then goes steeply to minus infinity. This is a consequence of the violation of the Pauli principle. In inset (c) of Fig. 1 we present the curves of the energy for $\kappa = 0.2$ MeV. This value lies beyond the phase transition, which is clearly seen in all the expectation values of the Dyson boson mapped Hamiltonian of Eq. (15). The three curves show a minimum at approximately $\rho = 1.7$ and are very close up to this point. After that, the exponential curve rises again and then decreases. The QRPA approximation is unable to go beyond the phase transition point. It just changes the sign of curvature, and the extremal point at $\rho = 0$ is a maximum. This feature is the so-called collapse of

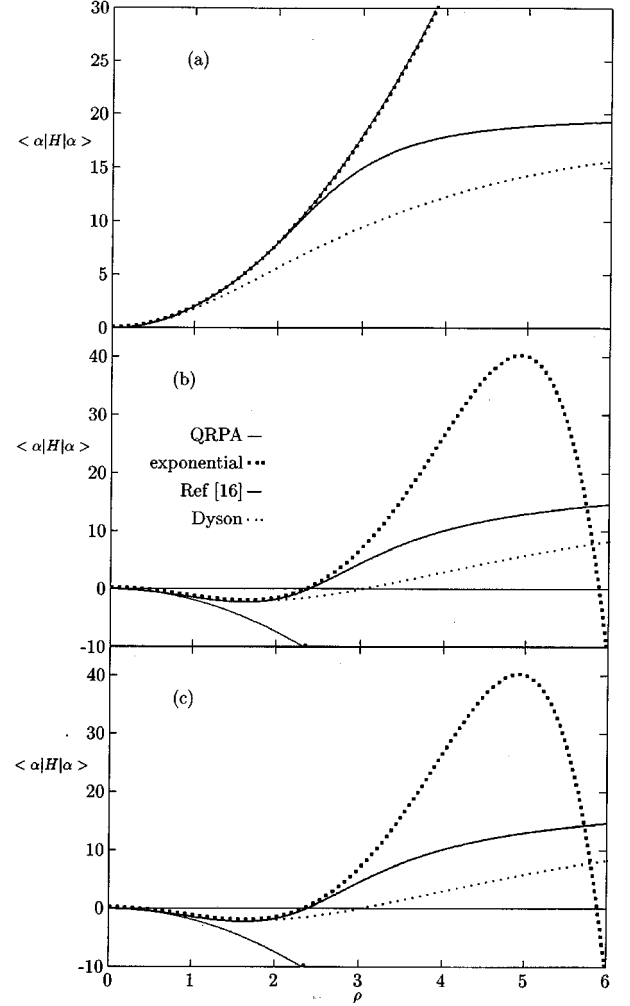


FIG. 1. Expectation value of the Hamiltonian as a function of the order parameter ρ . The expectation value $\langle \alpha_\infty | H_{\text{QRPA}} | \alpha_\infty \rangle$ is denoted by ‘‘QRPA,’’ $\langle \alpha_\infty | H | \alpha_\infty \rangle$ by ‘‘exponential,’’ $\langle \alpha | H | \alpha \rangle$ by ‘‘Ref. [16],’’ and $\langle \alpha | H | \tilde{\alpha} \rangle$ by ‘‘Dyson.’’ Insets (a), (b), and (c) show the results for $\kappa = 0, 0.1$, and 0.2 , respectively.

the QRPA [19]: if the eigenvalue goes to zero so does the coefficient of ρ^2 in $\langle \alpha_\infty | H_{\text{QRPA}} | \alpha_\infty \rangle$. When this coefficient becomes negative the energy becomes purely imaginary. Saturation properties due to the Pauli principle are shown by the curves quoted as ‘‘Ref. [16],’’ and ‘‘Dyson,’’ of Fig. 1, for large values of ρ . In the limit $\rho \rightarrow \infty$ the expectation value $\langle H \rangle \rightarrow 4\Omega\epsilon + \lambda_1$.

Figure 2 shows details around the minimum, in a larger scale. It includes the results for $\langle \alpha | H_{\text{QRPA}} | \alpha \rangle$, denoted ‘‘RQRPA.’’ It is thus clear that any approximation for the trial states, even the simplest exponential one, is able to detect the phase transition when applied to the exact Hamiltonian. While the exponential approximation fails for large values of ρ it works fine in the region around the deformed minimum. The differences between the Dyson approximation and the other curves beyond the minimum are noticeable. On the other side, the expectation value of the renormalized QRPA Hamiltonian describes a minimum with half the energy and at $\rho \approx 1.1$ which is far from the exact value.

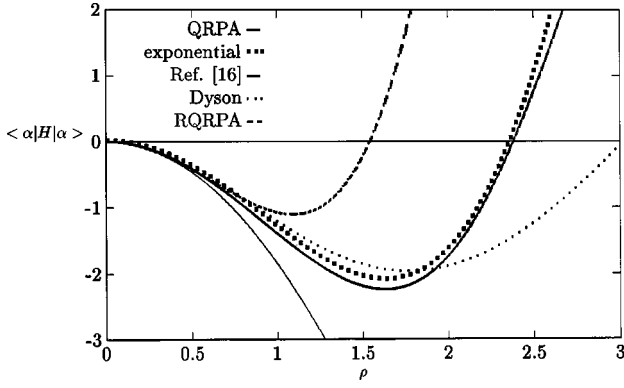


FIG. 2. Amplified version of Fig. 1, inset (c). Results for $\langle \alpha | H_{\text{RQRPA}} | \alpha \rangle$, denoted by ‘RQRPA’ are also included.

The modulus of the order parameter (ρ) at the minimum of $\langle H \rangle$ is shown in Fig. 3, as a function of the residual interaction parameter κ . In this plot the appearance of a phase transition is clearly observed. Up to $\kappa \sim 0.11$ MeV the minimum occurs for a coherent state with $\rho = 0$, i.e., the boson vacuum. From that point on instabilities dominate. The use of only an even number of bosons in the coherent state washes out the phase transition. For this case it is better to analyze the results shown in Fig. 4, where the value of $\langle H \rangle$ at the minimum is shown as a function in κ . While for the approximations which include all powers of b^\dagger the minimum lies at zero energy, up to the point where the phase transition occurs, using only even powers of b^\dagger produces an energy which is nearly constant up to the phase transition point. Afterwards it becomes a fast decreasing function.

The dependence of the expectation value of the number of proton-neutron pairs as a function of ρ is shown in Fig. 5. The saturation properties discussed in relation with the energy, Fig. 1, are also seen here. As the order parameter ρ increases, the number of bosons approaches its maximal value 2Ω , which is a consequence of Pauli principle. The exponential approximation has no truncation in the sum, thus it does not lead to a saturation but rather behaves quadratically as a function of ρ . Notice that for practical purposes all the approximations yield similar results up to $\rho \leq 2$, which implies that for these values the violation of the Pauli prin-

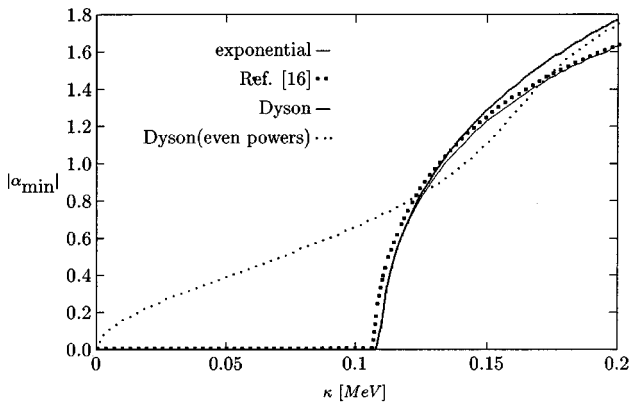


FIG. 3. The order parameter $\rho = |\alpha|$ at the minimum of $\langle H \rangle$, as a function of the residual interaction parameter κ . The meaning of the different approximations used is explained in the text.

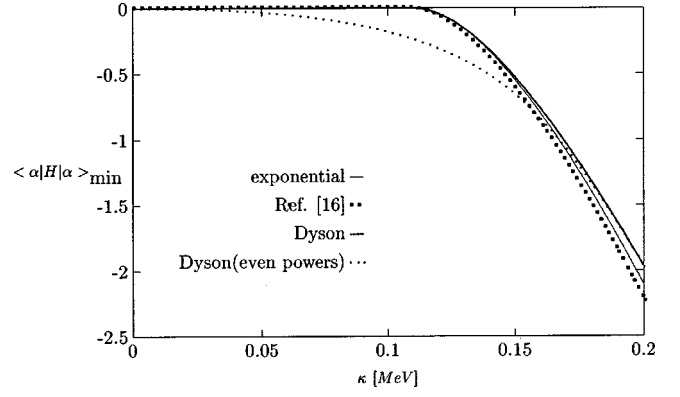


FIG. 4. The value of $\langle H \rangle$ at the minimum vs κ .

ciple do not influence the results significantly. However, Pauli principle violation effects dominate for larger values of ρ . Please also note that the position of the deformed minimum is located at $\rho < 2$ (see Fig. 1). Thus, the Pauli principle can be ignored for situations where the minimum occurs at values of ρ corresponding to an average occupation number smaller than half the filled shell.

Finally, Fig. 6 shows results for transitions induced by the Fermi β^- operator [see Eq. (32)]. The results are presented as a function of ρ [inset (a)] and κ [inset (b)]. The approximations used are the Dyson boson mapping with all powers included [see Eq. (21)] and the expansions corresponding to even and odd powers [see Eqs. (22) and (23)]. While the normalization factors N_0 , \tilde{N}_0 , $N_e \rightarrow 1$ when $\rho \rightarrow 0$, the normalization factor $N_o \rightarrow \rho^{-1}$. It explains the difference observed at the right-hand side of inset (a) of Fig. 6, where $\langle \alpha | \beta^- | \tilde{\alpha} \rangle \rightarrow 0$ when $\rho \rightarrow 0$ while $\langle \alpha_o | \beta^- | \tilde{\alpha}_e \rangle \rightarrow \text{const}$. As a consequence of the different behavior of $|\alpha_{\text{min}}|$, displayed in Fig. 3 for the different approximations considered, we have very distinct beta amplitudes. Having only odd or even powers of b^\dagger in the coherent state produces a large beta amplitude for all nonzero values of κ , as displayed in inset (b) of Fig. 6. The inclusion of all powers shows more clearly the presence of a phase transition. Since the matrix elements of the β^- operator [see Eqs. (33) and (34)] are directly related to the order parameter ρ , they acquire nonzero values only after the onset of the phase transition.

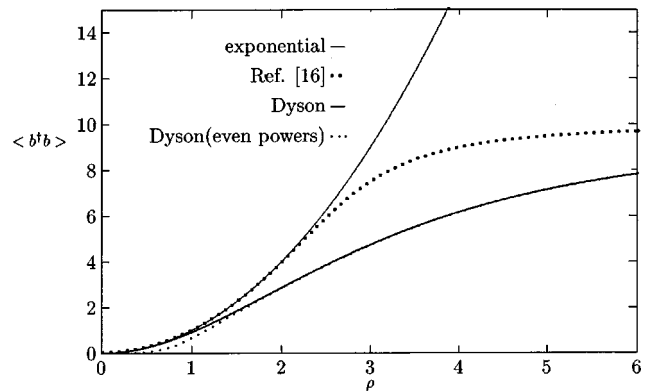


FIG. 5. The expectation value of the number of proton-neutron pairs as a function of ρ .

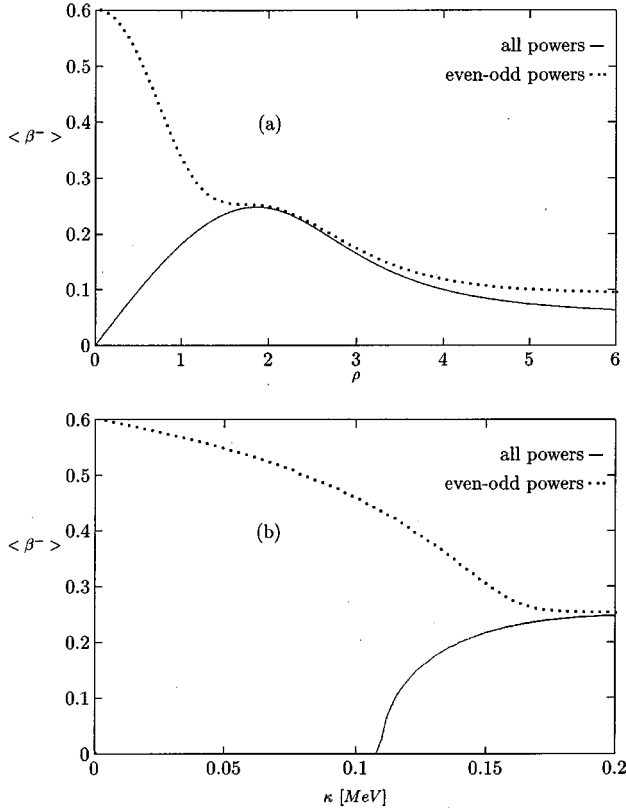


FIG. 6. The Fermi beta transition amplitude, both as a function of ρ [inset (a)] and κ [inset (b)]. The curves represent results obtained with the Dyson approximation with all boson powers included (solid line) and only even-odd powers (dotted lines).

Before closing this section we would like to comment on the comparison between exact results and the results of the above discussed approximations. The equivalence between a purely fermionic calculation and the one corresponding to Dyson boson mapping is fairly obvious, owing to the fact that the mapping preserves the commutation relations among the operators entering in the Hamiltonian and in the basis. As we have shown with the examples given in the previous subsections, the use of a variational approach and a nonperturbative expansion in the space of parameters yields solutions which are functions of the order parameter. The question which we are addressing now concerns the accuracy of the procedure. Table I shows the results of the different approximations discussed in the text, for the expectation value of the Hamiltonian. At first glance the results corresponding to the exponential trial state and to different terms of the Dyson boson mapping compare favorably with the exact results. However, the exponential set, as well as the set of Ref. [16], gives results which are below the exact ones. This unphysical behavior (i.e., the exact results should always be the lower bound of any approximation) is clearly seen for large κ values. On the other side the results of the Dyson boson mapping, particularly for the case of the expansion with even powers of the boson operator, yield very good results as compared with the exact ones. In this sense this approximation is equivalent to Hartree-Fock. The results shown in Table I are a good answer to the question of the accuracy of

TABLE I. Expectation value of the Hamiltonian $\langle H \rangle$, as a function of the residual interaction parameter κ .

κ	$\langle \alpha H \alpha \rangle$	$\langle \alpha_\infty H \alpha_\infty \rangle$	$\langle \alpha H \tilde{\alpha} \rangle$	$\langle \alpha_e H \tilde{\alpha}_e \rangle$	Exact
0.000	0.0000	0.0000	0.0000	0.0000	0.00000
0.010	0.0000	0.0000	0.0000	-0.0011	-0.00108
0.020	0.0000	0.0000	0.0000	-0.0045	-0.00454
0.030	0.0000	0.0000	0.0000	-0.0107	-0.01075
0.040	0.0000	0.0000	0.0000	-0.0201	-0.02015
0.050	0.0000	0.0000	0.0000	-0.0331	-0.03333
0.060	0.0000	0.0000	0.0000	-0.0504	-0.05101
0.070	0.0000	0.0000	0.0000	-0.0729	-0.07416
0.080	0.0000	0.0000	0.0000	-0.1014	-0.10403
0.090	0.0000	0.0000	0.0000	-0.1375	-0.14228
0.100	0.0000	0.0000	0.0000	-0.1827	-0.19114
0.110	-0.0044	-0.0001	-0.0001	-0.2392	-0.25353
0.120	-0.0704	-0.0435	-0.0430	-0.3102	-0.33330
0.130	-0.2033	-0.1567	-0.1533	-0.3996	-0.43510
0.140	-0.3903	-0.3264	-0.3167	-0.5133	-0.56408
0.150	-0.6220	-0.5427	-0.5225	-0.6592	-0.72487
0.160	-0.8908	-0.7977	-0.7627	-0.8466	-0.92023
0.170	-1.1910	-1.0855	-1.0312	-1.0797	-1.15008
0.180	-1.5178	-1.4011	-1.3235	-1.3515	-1.41173
0.190	-1.8675	-1.7407	-1.6356	-1.6523	-1.70100
0.200	-2.2368	-2.1010	-1.9646	-1.9748	-2.01345

the procedure, concerning the convergence to results which are a very good representation of the exact ones. The power of the expansion to detect phase transitions is also evident from the previously discussed results. Both features enable us to conclude about the suitability of the method to handle some specific features of many body Hamiltonians, like the one related to phase transitions in the space of parameters of the Hamiltonian.

VI. CONCLUSIONS

In the present work we have described the combined application of the Dyson boson mapping technique and the use of a coherent state representation to characterize phase transitions associated to a schematic Hamiltonian. We have introduced a complex order parameter and shown that the occurrence of phase transitions is linked to sudden changes in the value of the order parameter. The sensitivity of the energy, with respect to changes in the order parameter ρ used to determine the validity of the harmonic approximation (QRPA) and of its renormalized version (renormalized QRPA). In the present example, the number of proton-neutron pairs in vacuum was represented in terms of a complex order parameter. The spontaneous breaking of the proton-neutron-pair symmetry was induced by particle-particle interactions ($\kappa \neq 0$) and it manifests itself in the appearance of a zero-energy state. At this point, the analogy with the situation found in systems with permanent intrinsic deformations can be established [20]. We have shown that the renormalized QRPA is unable to describe correctly the energy and that the inclusion of the Pauli principle at the

Hamiltonian level is crucial to describe the phase transition. It was shown that very crude representations based on a coherent state are able to describe the phase transition, provided that the boson mapping of the Hamiltonian is performed to all orders. This results are relevant in the context of the coherent state description of systems based on the $SO(5)$ and $SO(8)$ algebras [10,11]. Work is in progress concerning the use of the present method in realistic situations.

ACKNOWLEDGMENTS

J.G.H. is on sabbatical leave from Departamento de Física, Centro de Investigación y de Estudios Avanzados del IPN. This work has been partially supported by the CONACYT (Mexico), the CONICET (Argentina) and the project PMT-PICT0079. Discussions with J. Dukelsky concerning the use of the Dyson coherent state are gratefully acknowledged.

-
- [1] P. Vogel and M. R. Zirnbauer, *Phys. Rev. Lett.* **57**, 3148 (1986).
 - [2] O. Civitarese, A. Faessler, and T. Tomoda, *Phys. Lett. B* **194**, 11 (1987).
 - [3] M. K. Moe and P. Vogel, *Annu. Rev. Nucl. Part. Sci.* **44**, 247 (1994).
 - [4] J. Suhonen and O. Civitarese, *Phys. Rep.* **300**, 124 (1998).
 - [5] P. Ring and P. Schuck, *The Nuclear Many-Body Problem* (Springer-Verlag, New York, 1980).
 - [6] D. J. Rowe, *Nuclear Collective Motion* (Methuen, London, 1970).
 - [7] F. Catara, N. Dinh Dang, and M. Sambataro, *Nucl. Phys.* **A579**, 1 (1994).
 - [8] A. M. Lane and J. Martorell, *Ann. Phys. (N.Y.)* **129**, 273 (1980).
 - [9] E. Caurier, A. Poves, and A. P. Zuker, *Phys. Lett. B* **252**, 13 (1990); E. Caurier, F. Nowacki, A. Poves, and J. Retamosa, *Phys. Rev. Lett.* **77**, 1954 (1996).
 - [10] J. G. Hirsch, P. O. Hess, and O. Civitarese, *Phys. Rev. C* **54**, 1976 (1996); *Phys. Lett. B* **390**, 36 (1997); *Phys. Rev. C* **56**, 199 (1997).
 - [11] J. Engel *et al.*, *Phys. Rev. C* **55**, 1781 (1997).
 - [12] A. Klein and E. R. Marshalek, *Rev. Mod. Phys.* **63**, 375 (1991).
 - [13] K. T. Hecht, *Vector Coherent State Method and its Application to Problems of Higher Symmetries*, Lecture Notes in Physics (Springer-Verlag, Heidelberg, 1987).
 - [14] V. A. Kuz'min and V. G. Soloviev, *Nucl. Phys.* **A486**, 118 (1988).
 - [15] O. Civitarese and J. Suhonen, *Nucl. Phys.* **A578**, 62 (1994).
 - [16] O. Civitarese, P. O. Hess, and J. G. Hirsch, *Phys. Lett. B* **412**, 1 (1997).
 - [17] A. Bohr and B. R. Mottelson, *Nuclear Structure V II* (Benjamin, Reading, MA, 1975).
 - [18] J. Toivanen and J. Suhonen, *Phys. Rev. Lett.* **75**, 410 (1995).
 - [19] O. Civitarese, A. Faessler, J. Suhonen, and X. R. Wu, *J. Phys. G* **17**, 943 (1991).
 - [20] D. R. Bes and J. Kurchan, *The Treatment of Collective Coordinates in Mechanical Systems; an Application to the BRST Invariance*, Vol. 34 of *Lecture Notes in Physics* (World Scientific, Singapore, 1990).